discussed on the basis of new experiment in future study.

Conclusions

From the viewpoint of adaptive multimode lubrication, the effectiveness of biphasic lubrication in natural synovial joints was examined by biphasic FE analyses under on–off loading and continuous loading to cartilage. The effectiveness of biphasic lubrication under on–off loading (migrating contact area) condition was clearly shown. For thin film condition for articular cartilage under continuous loading, the influence of adsorbed film formation was examined in experimental reciprocating test including restarting test after interruption and unloading, where the importance of rehydration and lubricant composition was indicated. Finally, the effectiveness of fibre reinforcement in PVA hydrogel was shown in the walking simulator test to be related to the biphasic mechanism.

Funding

This work was supported by the Grant-in-Aid for Specially Promoted Research of Japan Society for the Promotion of Science (grant no. 23000011).

Acknowledgements

The author thank his research members, particularly, Dr T Sakai, Kyushu Institute of Technology, for help with the biphasic FE analyses and simulator tests, Dr S Yarimitsu, Dr K Nakashima and Professor Y Sawae, Kyushu University, for cooperation in evaluation of friction properties in articular and artificial cartilages. He also thanks the organizing members for the invitation for the opening lecture to the 38th Leeds–Lyon Symposium on Tribology.

References

1. Willert HJ and Semlitsch M. Reaction of the articular capsule to wear products of artificial joint prostheses. *J Biomed Mater Res* 1977; 11: 157–164.
2. Ingham E and Fisher J. The role of macrophages in osteolysis of total joint replacement. *Biomaterials* 2005; 26: 1271–1286.
3. Murakami T. The lubrication in natural synovial joints and joint prostheses. *JSME Int J Ser III* 1990; 33(4): 465–474.
4. Dowson D. Modes of lubrication in human joints. *Proc IMechE Part J: J Engineering Tribology* 1966–1967; 181(3): 45–54.
5. Murakami T, Ohtsuki N, Chikama H, et al. Tribological study using human joint models. In: *Proceedings of the 8th international congress of biomechanics*, Nagoya, Japan, 5–6 November 1983, pp.97–104.
6. Dowson D and Jin ZM. Micro-elastohydrodynamic lubrication of synovial joints. *Eng Med* 1986; 15: 65–67.
7. McCutchen CW. The frictional properties of animal joints. *Wear* 1962; 5: 1–17.
8. Walker PS, Dowson D, Longfield MD, et al. Boosted lubrication in synovial joints by fluid entrapment and enrichment. *Ann Rheum Dis* 1968; 27(6): 512–520.
9. Swann DA. Macromolecules of synovial fluid. In: L Sokoloff (ed.) *The joints and synovial fluids*. vol. 1. New York: Academic Press, 1978, pp.407–435.
10. Higaki H and Murakami T. Role of constituents in synovial fluid and surface layer of articular cartilage in joint lubrication (part 2) the boundary lubricating ability of proteins. *Jpn J Tribol* 1996; 40(7): 691–699.
11. Hills BA. Oligolamellar lubrication of joints by surface active phospholipids. *J Rheumatol* 1989; 16(1): 82–91.
12. Murakami T, Sawae Y, Horimoto M, et al. Role of surface layers of natural and artificial cartilage in thin film lubrication. In: Dowson D, Priest M, Taylor CM, Ehret P, Childs THC, Dalmaz G, Berthier Y, Flamand L, Georges J-M and Lubrecht AA (eds) *Lubrication at frontier*. Amsterdam: Elsevier, 1999, pp.737–747.
13. Higaki H, Murakami T, Nakanishi Y, et al. The lubricating ability of biomembrane models with dipalmitoyle phosphatidylcholine and γ-Globulin. *Proc IMechE Part H: J Engineering in Medicine* 1998; 212: 337–346.
14. Murakami T, Higaki H, Sawae Y, et al. Adaptive multimode lubrication in natural synovial joints and artificial joints. *Proc IMechE Part H: J Engineering in Medicine* 1998; 212: 23–35.
15. Ateshian GA. Theoretical formulation for boundary friction in articular cartilage. *J Biomech Eng* 1997; 119(1): 81–86.
16. Ikeuchi K. Origin and future of hydration lubrication. *Proc IMechE Part J: J Engineering Tribology* 2007; 221: 301–305.
17. Klein J. Molecular mechanisms of synovial joint lubrication. *Proc IMechE Part J: J Engineering Tribology* 2006; 220: 691–710.
18. Zappone B, Ruths M, Greene WG, et al. Adsorption, lubrication, and wear of lubricin on model surfaces: polymer brush-like behavior of a glycoprotein. *Biophys J* 2007; 92: 1693–1708.
19. Ateshian GA, Wang H and Lai WM. The role of interstitial fluid pressurization and surface porosities on the boundary friction of articular cartilage. *ASME J Tribology* 1998; 120: 241–248.
20. Forster H and Fisher J. The influence of continuous sliding and subsequent surface wear on the friction of articular cartilage. *Proc IMechE Part H: J Engineering in Medicine* 1999; 213(4): 329–345.
21. Ateshian GA. The role of interstitial fluid pressurization in articular cartilage lubrication. *J Biomech* 2009; 42: 1163–1176.
22. Mow VC, Kuei SC, Lai WM, et al. Biphasic creep and stress relaxation of articular cartilage in compression theory and experiment. *J Biomech Eng* 1980; 102: 73–84.
23. Sakai N, Hagihara Y, Furusawa T, et al. Analysis of biphasic lubrication of articular cartilage loaded by cylindrical indenter. *Tribol Int* 2012; 46: 225–236.
24. Murakami T, Nakashima K, Sawae Y, et al. Roles of adsorbed film and gel layer in hydration lubrication for articular cartilage. *Proc IMechE Part J: J Engineering Tribology* 2009; 223: 287–295.

25. Murakami T, Nakashima K, Yarimitsu S, et al. Effectiveness of adsorbed film and gel layer in hydration lubrication as adaptive multimode lubrication mechanism for articular cartilage. *Proc IMechE Part J: J Engineering Tribology* 2011; 225: 1174–1185.
26. Williams PA, Yamamoto K, Masaoka T, et al. Highly crosslinked polyethylenes in hip replacements: improved wear performance or paradox? *Tribol Trans* 2007; 50: 277–290.
27. Tomita N, Kitakura T, Onmori N, et al. Prevention of fatigue cracks in ultrahigh molecular weight polyethylene joint components by the addition of vitamin E. *J Biomed Mater Res Part B* 1999; 48: 474–478.
28. Moro T, Takatori Y, Ishihara K, et al. Surface grafting of artificial joints with a biocompatible polymer for preventing periprosthetic osteolysis. *Nat Mater* 2004; 3: 829–836.
29. Issac GH, Thompson J, Williams S, et al. Metal-on-metal bearings surfaces: materials, manufacture, design, optimization, and alternatives. *Proc IMechE Part H: J Engineering in Medicine* 2006; 220: 119–133.
30. Früh HJ, Willmann G and Pfaff HG. Wear characteristics of ceramic-on-ceramic for hip endoprostheses. *Biomaterials* 1997; 18: 873–876.
31. Unsworth A, Pearcy MJ, White EFT, et al. Soft layer lubrication of artificial hip joints. *Proc IMechE Part C: J Mechanical Engineering Science* 1987; 219(87): 715–724.
32. Murakami T, Sawae Y, Higaki H, et al. Adaptive multimode lubrication in knee prostheses with artificial cartilage during walking. In: Dowson D, Taylor CM, Childs THC, Dalmaz G, Berthier Y, Flamand L, Georges J-M and Lubrecht AA (eds) *Elastohydrodynamics '96: Fundamentals and applications in lubrication and traction*. Amsterdam: Elsevier Science, 1997, pp.371–382.
33. Sasada T. Biomechanics and biomaterials–friction behaviour of an artificial articular cartilage. In: *Transactions of the 3rd world biomaterials congress*, Kyoto, Japan, 21–25 April 1988, vol. 11, p.6.
34. Oka M, Ushio K, Kumar P, et al. Development of artificial cartilage. *Proc IMechE Part H: J Engineering in Medicine* 2000; 214: 59–68.
35. Nakashima K, Sawae Y and Murakami T. Study of wear reduction mechanisms of artificial cartilage by synergistic protein boundary film formation. *JSME Int J* 2005; 48(4): 555–561.
36. Yarimitsu S, Nakashima K, Sawae Y, et al. Study on mechanisms of wear reduction of artificial cartilage through in situ observation on forming protein boundary film. *Tribol Online* 2007; 2(4): 114–119.
37. Yarimitsu S, Nakashima K, Sawae Y, et al. Effect of lubricant composition on adsorption behavior of proteins on rubbing surface and stability of protein boundary film. *Tribol Online* 2008; 3(4): 238–242.
38. Yarimitsu S, Nakashima K, Sawae Y, et al. Influence of lubricant composition on forming boundary film composed of synovia constituents. *Tribol Int* 2009; 42: 1615–1623.
39. Kobayashi M, Chang YS and Oka M. A two year in vivo study of polyvinyl alcohol-hydrogel (PVA-H) artificial meniscus. *Biomaterials* 2005; 26: 3243–3248.
40. Nakashima K, Sawae Y, Tsukamoto N, et al. Wear behavior of an artificial cartilage material for hemiarthroplasty. In: *Proceedings of the 6th world congress of biomechanics, WCB 2010*, Singapore, 1–6 August. *IFMBE Proc* 2010; 31: 1169–1172.
41. Murakami T, Sakai N, Sawae Y, et al. Influence of proteoglycan on time-dependent mechanical behaviors of articular cartilage under constant total compressive deformation. *JSME Int J Ser C* 2004; 47: 1049–1055.
42. Hosoda N, Sakai N, Sawae Y, et al. Depth-dependence and time-dependence in mechanical behaviors of articular cartilage unconfined compression test under constant total deformation. *J Biomech Sci Eng* 2008; 3(2): 209–220.
43. Jurvelin JS, Bushmann MD and Hunziker EB. Mechanical anisotropy of the human knee articular cartilage in compression. *Proc IMechE Part H: J Engineering in Medicine* 2003; 217: 215–219.
44. Li LP, Soulhat J, Buschmann MD, et al. Nonlinear analysis of cartilage in unconfined ramp compression using a fibril reinforced poroelastic model. *Clin Biomech* 1999; 14: 673–682.
45. Wu JZ, Herzog W and Epstein M. Evaluation of the finite element software ABAQUS for biomechanical modelling of biphasic tissues, technical note. *J Biomechanics* 1998; 31: 165–169.
46. Sakai N, Hosoda N, Hagiwara Y, et al. Analyses of functional mechanism of articular cartilage (in Japanese). *Biomechanisms* 2012; 21: 251–263.
47. Murakami T, Sawae Y, Nakashima K, et al. Micro- and nanoscopic biotribological behaviours in natural synovial joints and artificial joints. *Proc IMechE Part J: J Engineering Tribology* 2007; 221: 237–245.
48. Pawaskar SS, Jin ZM and Fisher J. Modelling of fluid support inside articular cartilage during sliding. *Proc IMechE Part J: J Engineering Tribology* 2007; 221: 165–174.
49. Murakami T, Yarimitsu S, Nakashima K, et al. Time-dependent frictional behaviours in hydorogel artificial cartilage materials. In: *Proceedings of the 6th international biotribology forum (Biotribology Fukuoka 2011)*, Fukuoka, Japan, 5 November 2011, pp.65–68.
50. Nakashima K, Sawae Y and Murakami T. Influence of protein conformation on frictional properties of poly (vinyl alcohol) hydrogel for artificial cartilage. *Tribol Lett* 2007; 26: 145–151.

Biochemical and Biophysical Research Communications 424 (2012) 724–729

Contents lists available at SciVerse ScienceDirect

Biochemical and Biophysical Research Communications

journal homepage: www.elsevier.com/locate/ybbrc

Effects of both vitamin C and mechanical stimulation on improving the mechanical characteristics of regenerated cartilage

Seiji Omata [a,*], Shogo Sonokawa [b], Yoshinori Sawae [c], Teruo Murakami [d]

[a] Department of Biomedical Engineering, Graduate School of Biomedical Engineering, Tohoku University, Sendai, Miyagi, Japan
[b] Department of Mechanical Engineering, Graduate School of Engineering, Kyushu University, Fukuoka, Japan
[c] Department of Mechanical Engineering, Faculty of Engineering, Kyushu University, Fukuoka, Japan
[d] Advanced Biomaterials Division, Research Center for Advanced Biomechanics, Kyushu University, Fukuoka, Japan

ARTICLE INFO

Article history:
Received 22 June 2012
Available online 16 July 2012

Keywords:
Regenerated-cartilage tissue
Interconnection
Extracellular matrix network
Mechanical property
Mechanical stimulation

ABSTRACT

The present work describes the influence of both vitamin C (VC) and mechanical stimulation on development of the extracellular matrix (ECM) and improvement in mechanical properties of a chondrocyte–agarose construct in a regenerating tissue disease model of hyaline cartilage. We used primary bovine chondrocytes and two types of VC, ascorbic acid (AsA) as an acidic form and ascorbic acid 2-phosphate (A2P) as a non-acidic form, and applied uniaxial compressive strain to the tissue model using a purpose-built bioreactor. When added to the medium in free-swelling culture conditions, A2P downregulated development of ECM and suppressed improvement of the tangent modulus more than AsA. By contrast, application of mechanical stimulation to the construct both increased the tangent modulus more than the free-swelling group containing A2P and enhanced the ECM network of inner tissue to levels nearly as high as the free-swelling group containing AsA. Thus, mechanical stimulation and strain appears to enhance the supply of nutrients and improve the synthesis of ECM via mechanotransduction pathways of chondrocytes. Therefore, we suggest that mechanical stimulation is necessary for homogenous development of ECM in a cell-associated construct with a view to implantation of a large-sized articular cartilage defect.

1. Introduction

Articular cartilage covers the surface of the ends of bones in synovial capsules and performs the important function of high performance weight-bearing at very low friction and wear in daily activities during a healthy life. The behavior of articular cartilage tissue as a mechanical system is dependent chiefly on an extracellular matrix (ECM), which consists primarily of a protein, called type II collagen (10–20% of the wet weight), and proteoglycans (about 10% of the wet weight) [1]. Steric and electrostatic interactions of ECM molecules in the cartilage tissue occur between the cationic collagen fibers and the anionic proteoglycans to provide a highly charged environment under neutral pH conditions. Although adult articular cartilage is a remarkable load-bearing system, following traumatic injury or under conditions of wear and tear, it lacks the ability of self-repair, which can often lead to osteoarthritis (OA).

Such diseases of hyaline cartilage are a major health problem, especially in industrialized countries with relatively long active life expectancies. At present, no cell-assisted tissue regeneration therapy for the reliable and durable replacement of damaged articular cartilage has been established [2–4]. However, in recent years, tissue engineering has become a promising option for the treatment of OA and has allowed researchers to produce functional replacements for diseased cartilage [5,6]. Developments in therapeutic strategies for damaged cartilage treatment have increasingly focused on the promising technology of cell-assisted repair, which proposes the use of autologous chondrocytes or other cell types to regenerate articular cartilage [4,7].

There is still too little knowledge available to establish a suitable design strategy for reconstructing tissue-engineered cartilage that matches the mechanical properties of natural tissue. In this study, we focused on the relationship between the collagen network and the mechanical properties of a regenerated-cartilage tissue model and showed that the collagen network interconnecting chondrocytes improved the mechanical properties of the tissue to be equivalent to that of scaffold material without chondrocytes if there was no linkage between cells by the ECM network [8]. We used ascorbic acid (AsA), a type of vitamin C (VC), in the culture medium to control collagen synthesis in order to investigate the

* Corresponding author. Address: Sato-Huang/Deguchi Lab. Graduate School of Biomedical Engineering, Tohoku University, 6-6-1, Aoba, Aramaki, Aoba, Sendai, Miyagi 980-8579, Japan.
E-mail address: s_omata@bml.mech.tohoku.ac.jp (S. Omata).

0006-291X/$ - see front matter © 2012 Elsevier Inc. All rights reserved.
http://dx.doi.org/10.1016/j.bbrc.2012.07.019

effect of developing a collagen network on the mechanical properties of the tissue model. However, high concentrations of AsA were found to be toxic to the chondrocytes with no concomitant improvement in mechanical properties.

As for AsA above, we used ascorbic acid 2-phosphate (A2P), a non-acidic form, for suppressing the cytotoxicity and effective development of the mechanical characteristics of the tissue, and demonstrated the relationship between VCs in the culture medium and development of ECM and mechanical properties of the construct. In addition, we thought that applying a compressive deformation to the tissue model would not only improve diffusion of culture medium into the tissue and accelerate the supply of nutrients, but also activate cell-signaling via mechanosensor and mechanotransduction pathways. It is well known that loading mechanical stimuli to regenerated-cartilage tissue and chondrocytes is distinctly important for both enhancing synthesis of ECM and inducing chondrogenesis differentiation of stem cells [9]. Hence, in order to apply a compressive deformation to the tissue model for development of ECM, we made a purpose-built bioreactor capable of applying an uniaxial unconfined compressive strain to individual constructs in an incubator. The purpose of the present study was to investigate the effects of applying both two types of VC and dynamic compression to a regenerated-cartilage tissue model on the mechanical properties and development of the ECM network.

2. Materials and methods

2.1. Sample preparation and tissue culture

Primary bovine chondrocytes were isolated from metacarpophalangeal joints of steers purchased from a butchery using a sequential enzyme digestion method [10]. Full thickness articular cartilage tissue was harvested from the proximal articular surface of the metatarsal bone and finely diced with a scalpel. The finely diced cartilage tissue was enzymatically digested in a 25 unit/mL protease solution (P8811, Sigma, St Louis, MO) for 3 h and subsequently in a 200 unit/mL collagenase solution (C7657, Sigma) for 18 h at 37 °C. Both enzyme solutions were prepared in sterile tissue culture medium consisting of Dulbecco's modified Eagle's medium (DMEM; D5921, Sigma) supplemented with 20 v/v% Fetal Bovine Serum (FBS; 10437–028, Gibco, Carlsbad, CA), 2 mM L-glutamine (G7513, Wako Pure Chemical Industries, Ltd., Osaka, Japan), 100 unit/mL penicillin, 100 μg/mL streptomycin, 0.25 μg/mL amphotericin B (161–23181, Wako), 20 mM Hepes (H0887, Sigma), and 0.85 mM L-ascorbic acid (AsA; A5960, Sigma). The supernatant of the resultant solution was centrifuged to separate chondrocytes at 40 × *g* for 5 min. The resultant cell pellet was washed twice in fresh culture medium, and then cell number and cell viability were determined using Trypan Blue assay. In this study, Sigma Type VII agarose (A6560, Sigma) was used to prepare a chondrocyte–agarose construct. The agarose powder was dissolved in Earle's Balanced Salts Solution (EBSS; Sigma) at twice the required final concentration (1 w/v%) and mixed with an equal volume of the cell suspension to yield the desired agarose concentration with a final cell density of 1×10^7 cells/mL. The molten cell-agarose solution was poured into an acrylic mold and quenched into gel at 4 °C for 30 min to create cylindrical constructs with a diameter of 4 mm and a height of 2.5 mm. The resultant cell-agarose constructs were placed into a 24-well culture plate and cultured with 1 mL culture medium in an incubator at 37 °C and 5% CO_2. The culture medium was exchanged every 2 days. Several culture media with different VC concentrations, from 2.2 to 32 pmol/10^9 cells, were prepared and used to evaluate the effect of AsA and L-ascorbic acid 2-phosphate magnesium salt (A2P, Wako) concentrations. Culture medium without VC was also used as a control. Each medium is abbreviated as AsA(2.2), A2P(6.4), and A2P(32) hereafter in this paper.

After 1 day of free-swelling culture, the constructs in the experiment group were subjected to uniaxial compression within a purpose-built bioreactor system as shown in Fig. 1. The system permits the application of strain independently in both vertical and horizontal directions to individual constructs using a 24-well plate in a commercially available incubator. The movements were controlled with respective linear variable displacement transducers and linear guide actuators. Strain was applied to the individual constructs through a loading plate, which was attached to the actuator via a jig. Uniaxial cyclic compression up to a maximum amplitude of 15% was applied in a triangular waveform at a frequency of 1 Hz for 6 h and subsequently off-loaded with the plate resting for each construct over the subsequent 18 h. Control constructs were cultured, in contrast, with both upper and lower plates for diffusion through the sides alone.

2.2. Measurement of mechanical property

To examine the influence of VC concentration, cell-agarose constructs were subjected to unconfined compression while immersed in culture medium at room temperature. Individual constructs were tested after culture periods of 22 days. Mechanical tests were

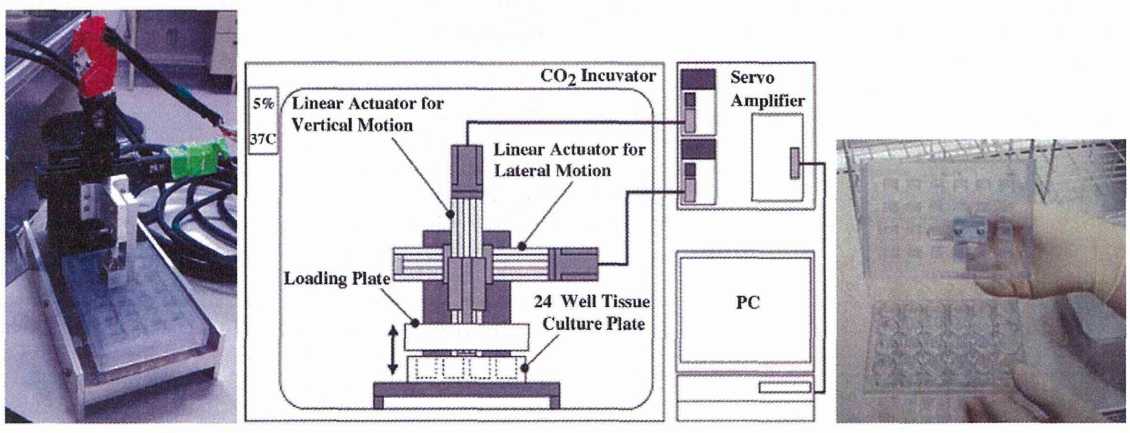

Fig. 1. Photograph (left) and Schematic drawing (center) of mechanical loading system mounted within tissue culture incubator. Loading plate with 22 plungers coupled with a 24-well culture plate (right).

performed with an impermeable stainless steel plunger at a strain rate of 0.5 mm/min up to a strain of 10%, while the load was recorded with a 10 N load sensor. The tangent modulus of the construct was calculated from the slope of a straight-line approximation of the stress–strain curve with a range of 0–15% strain using the least-square method.

2.3. Immunohistology

Separate constructs were used for trichrome immunofluorescence observation to examine the morphological characteristics of the elaborated ECMs, in particular type I collagen, type II collagen and chondroitin sulfate. After the prescribed culture periods, representative constructs were cut into slices with a thickness of approximately 1 mm using a knife. The slices were washed in PBS(−) and subsequently incubated in PBS(−) + 1 w/v% bovine serum albumin (BSA; Wako) for 30 min at 37 °C. These slices were incubated in PBS(−) containing the three monoclonal antibodies (bovine IgG1 isotype anti-type I collagen, Funakoshi, Tokyo, Japan; embryonic chicken IgG2a isotype anti-type II collagen, Funakoshi; mouse IgM isotype anti-chondroitin sulfate, Sigma) for 90 min at 37 °C to primarily label the collagens and the proteoglycan at once. The slices were then washed three times in PBS(−) for 10 min and incubated in PBS(−) containing the three secondary antibodies corresponding to each of the primary antibodies (Alexafluor 350-conjugated anti-mouse IgG1 antibody, A21120; Alexafluor 488-conjugated anti-mouse IgG2a antibody, A11001; Alexafluor 568-conjugated anti-mouse IgM antibody, A21043, Invitrogen) for 60 min at 37 °C. Labeled ECM molecules were fluorescently visualized within the cultured cell-agarose construct. The fluorescently stained specimens were mounted on the coverslip and observed using a confocal laser scanning microscope (CLSM; Eclipse; Nikon Corp., Tokyo, Japan).

2.4. Cell viability

The cell viability of individual constructs was assessed at different concentration of the VCs using a previously reported protocol [11]. The cultured constructs were cut into slices with a thickness of approximately 1 mm and washed in PBS(−) for 5 min at 37 °C. These slices were incubated in PBS(−) containing two fluorescent dyes (live cells: Calcein AM, Molecular Probes; dead cells: Ethidium homodimer-1, Molecular Probes) for 15 min at 37 °C. The fluorescently stained constructs were then washed by PBS(−) several times and mounted on the coverslip and observed by CLSM.

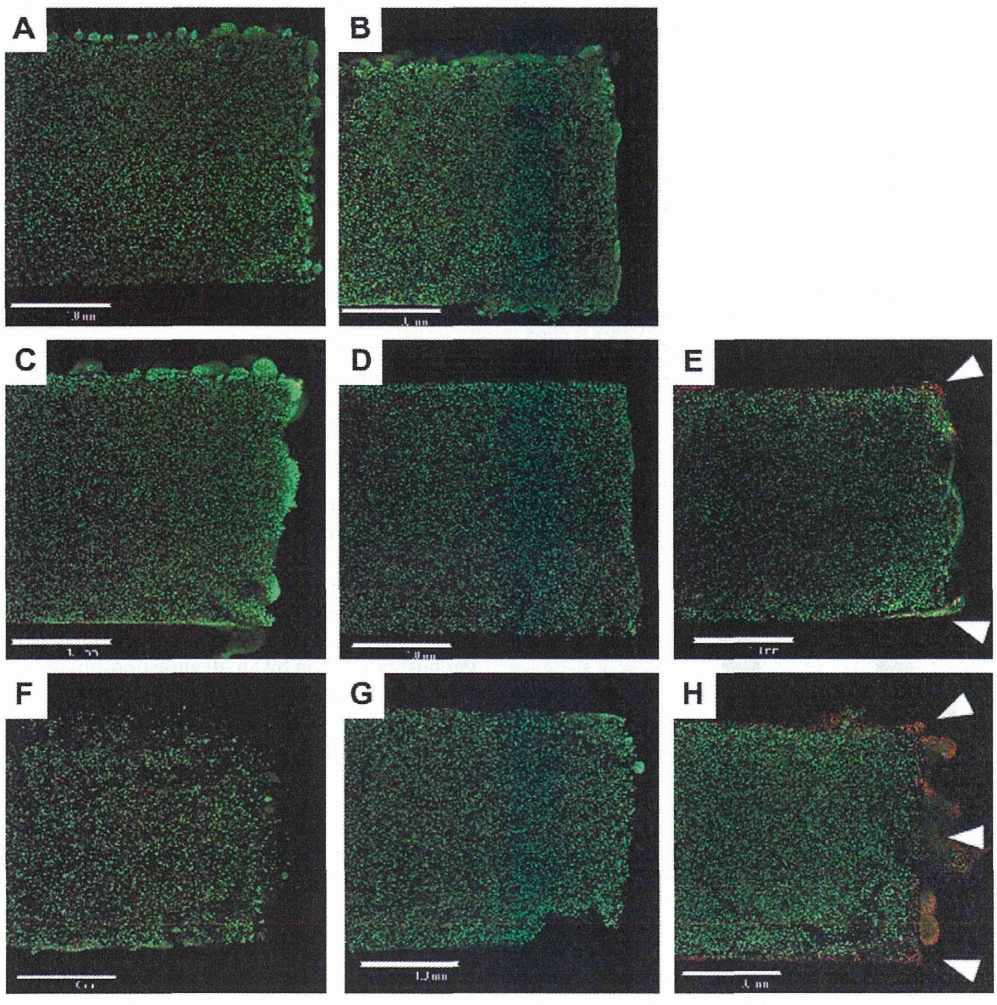

Fig. 2. Low-magnification immunofluorescence images of cell viability under free swelling (A, B, C, F), control (D, G) or compression (E, H) culture conditions. (A): without VC; (B): AsA(2.2); (C–E): A2P(6.4); (F–G): A2P(32). Green represents live cells and red represents dead cells. The culture period was 22 days. Each trichrome-stained sample represents an individual culture. The scale bar represents 1 mm.

2.5. Statistical analysis

Result of the tangent modulus were expressed as the mean ± sample standard deviation (*SD*). The significance of the difference between each experimental group was assayed using the two-tailed Welch's *t*-test. The degree of freedom was abbreviated to *df*. If the results of pairwise comparisons between two groups were *P*-value < 0.01, $d > 1$ and $(1 - \beta) > 0.8$ simultaneously, we judged the difference as significant in the tangent modulus, where *P*-value: level of significance; *d*: Cohen's *d*, an indicator of the effect size [12]; $(1 - \beta)$: the power of the test calculated by R language.

3. Results

3.1. Viability test

In the majority of cases there was a high degree of viability after 22 days of culture, as indicated in Fig. 2. However, some cytotoxicity was evident in the corner of the constructs in two experimental groups, namely A2P(6.4), and most particularly A2P(32), as indicated by the arrow-heads in Fig. 2(E) and (H).

3.2. Measurement of mechanical properties

To evaluate the influence of the mechanical stimulation on the cultured constructs, the tangent moduli of each group after 22 days of culture is shown in Fig. 3. Comparison within the four free-swelling groups only indicated significant differences between the without VC and the AsA(2.2) groups, the latter revealing an increased tangent modulus. By applying cyclic compression to the construct with addition of VC to the culture medium, there was not a clear difference between free-swelling and compression groups for AsA. By contrast, both tangent moduli of the two compression groups were higher than those of several free-swelling samples in each A2P dose group (A2P(6.4) and A2P(32)). Each tangent modulus of the control groups with A2P was ranked against the free-swelling and compression groups. It is not evident that there were differences between each pair of the three compression groups (AsA(2.2), A2P(6.4) and A2P(32)) (AsA(2.2), A2P(6.4): $df = 16$, $P = 0.47$, $d = 0.32$, $(1 - \beta) = 0.030$), but A2P(32) was lower than both AsA(2.2) and A2P(6.4) because each effect size (d) was large but each power ($(1 - \beta)$) was not (AsA(2.2), A2P(32): $df = 25$, $P = 0.017$, $d = 0.99$, $(1 - \beta) = 0.43$; A2P(6.4), A2P(32): $df = 15$, $P = 0.011$, $d = 1.3$, $(1 - \beta) = 0.54$).

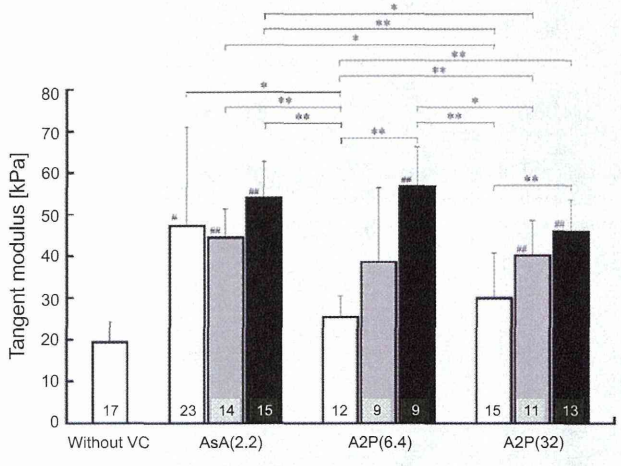

Fig. 3. Comparison of the tangent moduli after 22-day culture period. Cultures were terminated following free-swelling (white column), control (gray), or compression (black) conditions. Each number in the columns is the cultured sample number and each sample represents an individual culture. The error bar represents SD. Sharps (# and ##) and asterisks (* and **) show respective statistical significance between control group and each groups in Welch's *t*-test. #, *: $d > 1$, $P < 0.01$, $(1 - \beta) > 0.8$; ##, **: $d > 2$, $P < 0.01$, $(1 - \beta) > 0.8$.

3.3. Histological observation

Fig. 4 shows immunofluorescent images at low and high magnification revealing the ECM distribution (type I and II collagen and chondroitin sulfate) after 22 days. The high-magnification images were taken in the vicinity of the center of the construct. As indicated in Fig. 4(a) and (A), it is clear that with the absence of VC in the culture medium, there was only a limited amount of ECM. By contrast, in the free-swelling group (AsA(2.2)), there was a fairly uniform distribution of ECM across the construct (Fig. 4(b)). As indicated by the arrows in Fig. 4(B), at high magnification, this revealed a collagen network interconnected between chondrocytes. The low-magnification images for each of the A2P dose groups revealed a similar distribution in ECM across the constructs (Fig. 4(c)–(h)), although it was difficult to observe the ECM in the peripheral region of the compressed construct associated with group A2P(32), as indicated by the arrow-heads in Fig. 4(h). In the high magnification images, type II collagen seems to be interconnected between the chondrocytes, as indicated by the arrow in Figs. 4(E), (G) and (H). However, those examinations revealed that the compression groups of A2P(6.4) and A2P(32) were associated with a more abundant collagen network than the corresponding free-swelling groups. In addition, it is clearly evident that the distribution of chondroitin sulfate is restricted to the peripheral regions of the chondrocytes.

4. Discussion

In order to establish a suitable method for regenerating tissue-engineered cartilage, we studied the effects of two types of chemical and physical stimulations on the mechanical properties of the chondrocyte–agarose construct a regenerated-cartilage model. The first stimulation was the addition of high concentration of VC to the culture medium in order to enhance collagen synthesis. The second was the application of a compressive strain to the construct using a purpose-built bioreactor. Our results show that compressive strain had led to an increase in the tangent modulus and that the collagen network had become dense and interconnected among chondrocytes. We have already described the importance of chondrocyte linkage by ECM for the development of bulk elasticity of the construct in a previous study.

It is well known that even though A2P has no physiological activity, it can nevertheless reproduce the effect of VC activity after dephosphorylation by an alkaline phosphatase (ALP) [13]. Dephosphorylated A2P, or AsA, penetrates chondrocytes through a VC transporter, chiefly the sodium-dependent VC transporter 2 (SVCT2), and supports collagen synthesis as a cofactor in the rough endoplasmic reticulum [14]. In free-swelling culture conditions, we only observed a small number of collagen molecules distributed in the construct. We also observed that the tangent moduli of both A2P dose groups were lower than the moduli of AsA(2.2). We must also consider the reaction rates of both dephosphorylation of A2P by ALP and the transport of AsA into the cytosol via SVCT2. The Michaelis constants of bovine chondrocytes ALP and SVCT2 are 1–10 and 62 ± 25 μM, respectively [15,16]. The affinity of the substrate is slightly higher for ALP than for SVCT2, and as a result, AsA concentration around chondrocytes was lower in the A2P group. The rate of collagen synthesis was also relatively lower in the A2P group than the AsA dose group. Hence, the

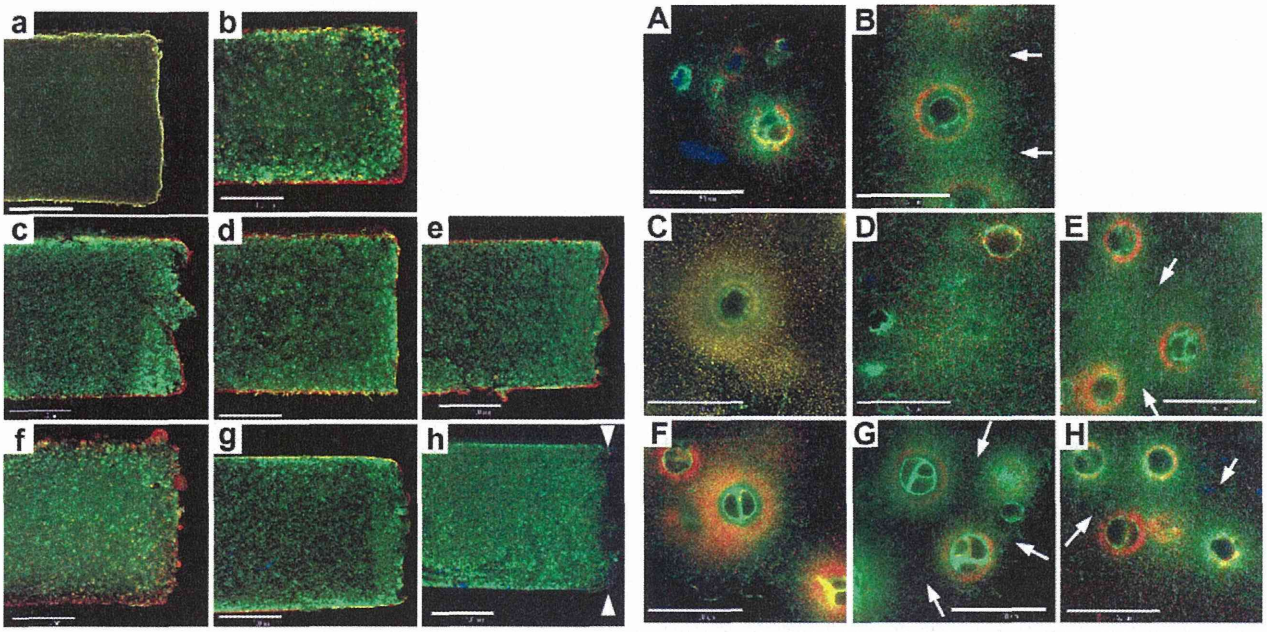

Fig. 4. Low- and high-magnification immunofluorescence images of ECMs under either free-swelling (a, b, c, f, A, B, C, F), control (d, g, D, G), or compression (e, h, E, H) culture conditions. (a, A): without VC; (b, B): AsA(2.2); (c–e, C–E): A2P(6.4); (f–g, F–G): A2P(32). Blue: type I collagen; green: type II collagen; red: chondroitin sulfate. The culture period was 22 days. Scale bars represent 1 mm (a–g) and 50 μm (A–G), respectively. Arrow-heads indicate that we could not observe ECMs at periphery of the tissue of compression group A2P(32). Arrows indicate interconnections among chondrocytes by type II collagen network.

tangent modulus of the free-swelling groups with A2P was suppressed by restraining cytotoxicity of AsA.

When applying compressive strain to the construct, each tangent modulus of A2P(6.4) and A2P(32) was higher than the moduli for the respective free-swelling groups. This is because the collagen network of these groups expanded, which allowed collagen fibers to interconnect among the chondrocytes. We think this mechanical stimulation enhanced diffusion of A2P and nutrients, homogenizing A2P within the construct. In addition, the stimulation probably excited a mechanosensor, activating cell-signaling pathways, namely the mechanotransduction pathways. It is well-known that mechanical stimulation causes chondrocytes to undergo several biological responses involving cartilage remodeling strategies that are relevant to the implantation of cultured tissue [17], e.g., activation of a mitogen-activated protein kinase (MAPK) pathway, a cell-signaling pathway [18,19], an increase in GAG biosynthesis [20], and regulation of inflammatory species synthesis [21]. These chondrocyte responses followed soon after mechanical stimulation and activity of the MAPK pathway was maintained for 5–60 min [18,19]. In synthesizing ECM with mechanical stimulation, chondrocytes built up the collagen network and adapted to changes in the deformation around the cells. Therefore, the compression group with A2P had a higher tangent modulus than the free-swelling group.

The tangent modulus of the compression group with A2P(32) tended to decrease more than the compression group of A2P(6.4) because ECM had been less developed in the peripheral region of A2P(32) than A2P(6.4). Moreover, viability observations revealed that cytotoxicity occurred at the peripheral regions of A2P(32). Generally, we can think that uniaxial compressive deformation of a cylinder model follows the same physics as two-dimensional tension in a plane perpendicular to the axial direction. When the tangent modulus is uniform in the construct, the force at the outer diameter position will be the largest because a reactive force is directly proportionate to the radius. Therefore, less ECM at the peripheral region induced a decrease in the tangent modulus of the construct.

As mentioned above, it is not easy to homogenously develop ECM in free-swelling culture conditions for the purpose of making large-sized regenerated-cartilage tissue. Based on the results of this study, it is necessary to apply mechanical strain to the construct because nutrients should be uniformly supplied. If we also consider the diffusion of nutrients under free-swelling culture conditions, we must note that the diffusion coefficient of water in agarose gel is about 10×10^{-10} m^2s [22,23]. Applying Fick's law, this means that a water molecule diffuses 10 mm per day in the gel. Pluen et al. reported that the diffusion coefficients of proteins in 0.1 M PBS(−) solution, lactalbumin and ovalbumin, were 0.8–1×10^{-10} m^2s [24], and therefore that nutrient particles diffuse 3 mm per day in the gel. Moreover, if the ECM of the cultured construct is dense, it is difficult for nutrients to diffuse in the tissue and the diffusion coefficient will be decreased. Thus, for clinical implantation of a large-sized regenerated-cartilage tissue in order to treat a cartilage defect, the construct should be prepared by applying mechanical stimulation, which would homogenously develop the ECM network.

In summary, this study investigated the influence of two types of VC, AsA and A2P, on the development of the ECM network and regulation of the mechanical properties of chondrocyte–agarose constructs. The collagen network of A2P dose groups improved more than the AsA dose group in free-swelling culture conditions and the tangent modulus of the A2P dose groups did not increase. Moreover, it is clear that free-swelling culture conditions suppressed development of ECM of the inner tissue more than the outer tissue. When applying compressive strain to the construct, tangent moduli of the A2P dose groups were higher due to the fact that ECM networks of the inner tissue had been upregulated with interconnections among the chondrocytes. Additionally, we propose that mechanical stimulation enhanced diffusion of nutrients and improved synthesis of the ECM via mechanotransduction

pathways. We conclude that the application of mechanical stimulation to a large-sized engineered-tissue is necessary for the treatment of articular cartilage defects of various sizes and forms.

Acknowledgments

This study was financially supported by the Grant-in-Aid for Scientific Research from the Japan Society for the Promotion of Science (20360078).

References

[1] R.M. Schulz, A. Bader, Cartilage tissue engineering and bioreactor systems for the cultivation and stimulation of chondrocytes, Eur. Biophys. J. 35 (2007) 539–568.
[2] A. Getgood, R. Brooks, L. Fortier, N. Rushton, Articular cartilage tissue engineering: today's research, tomorrow's practice?, J Bone Joint Surg. Br. 91 (2009) 565–576.
[3] S.R. Frenkel, P.E. Di Cesare, Scaffolds for articular cartilage repair, Ann. Biomed. Eng. 32 (1) (January 2004) 26–34.
[4] J. Farr, B. Cole, A. Dhawan, J. Kercher, S. Sherman, Clinical cartilage restoration: Evolution and overview, Clin. Orthop. Relat. Res. 469 (2011) 2696–2705.
[5] A.H. Gomoll, G. Filardo, L. de Girolamo, J. Esprequeira-Mendes, M. Marcacci, W.G. Rodkey, R.J. Steadman, S. Zaffagnini, E. Kon, Surgical treatment for early osteoarthritis. part I: cartilage repair procedures, Knee Surg. Sports Traumatol. Arthrosc. 20 (2012) 450–466.
[6] A.H. Gomoll, G. Filardo, F.K. Almqvist, W.D. Bugbee, M. Jelic, J.C. Monllau, G. Puddu, W.G. Rodkey, P. Verdonk, R. Verdonk, S. Zaffagnini, M. Marcacci, Surgical treatment for early osteoarthritis. part II: allografts and concurrent procedures, Knee Surg. Sports Traumatol. Arthrosc. 20 (2012) 468–486.
[7] C.M. Revell, K.A. Athanasiou, Success rates and immunologic responses of autogenic, allogenic, and xenogenic treatments to repair articular cartilage defects, Tissue Eng. Part B 15 (2009) 1–15.
[8] S. Omata, Y. Sawae, T. Murakami, Influence of ascorbic acid (asa) concentration in culture medium on mechanical property of regenerated cartilage, J. Environ. Eng. 6 (2011) 416–425.
[9] S. Grad, D. Eglin, M. Alini, M.J. Stoddart, Physical stimulation of chondrogenic cells in vitro: A review, Clin. Orthop. Relat. Res. 469 (2011) 2764–2772.
[10] D.A. Lee, D.L. Bader, Compressive strains at physiological frequencies influence the metabolism of chondrocytes seeded in agarose, J. Orthop. Res. 15 (1997) 181–188.
[11] M.M. Knight, S.R. Roberts, D.A. Lee, D.L. Bader, Live cell imaging using confocal microscopy induces intracellular calcium transients and cell death, Am. J. Physiol. Cell Physiol. 284 (2003) 1083–1089.
[12] J. Cohen, Statistical power analysis for the behavioral sciences, 2nd ed., Lawrence Erlbaum Assoc Inc., New Jersey, 1988.
[13] S. Takamizawa, Y. Maehata, K. Imai, H. Senoo, S. Sato, R. Hata, Effects of ascorbic acid and ascorbic acid 2-phosphate, a long-acting vitamin C derivative, on the proliferation and differentiation of human osteoblast-like cells, Cell Biol. Int. 27 (2004) 255–262.
[14] I. Savini, A. Rossi, C. Pierro, L. Avigliano, M.V. Catani, SVCT1 and SVCT2: key proteins for vitamin C uptake, Amino Acids 34 (2008) 347–355.
[15] A.L. McNulty, T.P. Vail, V.B. Kraus, Chondrocytenext term transport and concentration of ascorbic acid is mediated by SVCT2, Biochim. Biophys. Acta 1712 (2005) 212–221.
[16] R. Fortuna, H.C. Anderson, R.P. Carty, S.W. Sajdera, Enzymatic characterization of the chondrocytic alkaline phosphatase isolated from bovine fetal epiphyseal cartilage, Biochim. Biophys. Acta 570 (1979) 291–302.
[17] L. Ramage, G. Nuki, D.M. Salter, Signalling cascades in mechanotransduction: cell-matrix interactions and mechanical loading, Scand. J. Med. Sci. Sports 19 (2009) 457–469.
[18] J.B. Fitzgerald, M. Jin, D. Dean, D.J. Wood, M.H. Zheng, A.J. Grodzinsky, Mechanical compression of cartilage explants induces multiple time-dependent gene expression patterns and involves intracellular calcium and cyclic AMP, J. Biol. Chem. 279 (2004) 19502–19511.
[19] J.B. Fitzgerald, M. Jin, D.H. Chai, P. Siparsky, P. Fanning, A.J. Grodzinsky, Shear- and compressioninduced chondrocyte transcription requires MAPK activation in cartilage explants, J. Biol. Chem. 283 (2008) 6735–6743.
[20] J.D. Kisiday, J.H. Lee, P.N. Siparsky, D.D. Frisbie, C.R. Flannery, J.D. Sandy, A.J. Grodzinsky, Catabolic responses of chondrocyte-seeded peptide hydrogel to dynamic compression, Ann. Biomed. Eng. 37 (2009) 1368–1375.
[21] O.O. Akanji, P. Sakthithasan, D.M. Salter, T.T. Chowdhury, Dynamic compression alters NFκB activation and IκB-α expression in IL-1β-stimulated chondrocyte/agarose constructs, Inflamm. Res. 59 (2010) 41–52.
[22] E. Davies, Y. Huang, J.B. Harper, J.M. Hook, D.S. Thomas, I.M. Burgar, P.J. Lillford, Dynamics of water in agar gels studied using low and high resolution 1H NMR spectroscopy, Int. J. Food Sci. Technol. 45 (2010) 2502–2507.
[23] N.O. Gustafsson, B. Westrin, A. Axelsson, G. Zacchi, Measurement of diffusion coefficients in gels using holographic laser interferometry, Biotechnol. Progr. 9 (1993) 436–441.
[24] A. Pluen, P.A. Netti, R.K. Jain, D.A. Berk, Diffusion of macromolecules in agarose gels: comparison of linear and globular configurations, Biophys. J. 77 (1999) 542–552.

Colloids and Surfaces B: Biointerfaces 99 (2012) 1–6

Contents lists available at SciVerse ScienceDirect

Colloids and Surfaces B: Biointerfaces

journal homepage: www.elsevier.com/locate/colsurfb

Cell adhesion control on photoreactive phospholipid polymer surfaces

Batzaya Byambaa [a,c], Tomohiro Konno [a,*], Kazuhiko Ishihara [a,b,c]

[a] Department of Bioengineering, School of Engineering, The University of Tokyo, 7-3-1, Hongo, Bunkyo-ku, Tokyo 113-8656, Japan
[b] Department of Materials Engineering, School of Engineering, The University of Tokyo, 7-3-1, Hongo, Bunkyo-ku, Tokyo 113-8656, Japan
[c] School of Engineering and Center for Medical System Innovation, The University of Tokyo, 7-3-1, Hongo, Bunkyo-ku, Tokyo 113-8656, Japan

ARTICLE INFO

Article history:
Available online 7 September 2011

Keywords:
Stimuli-responsive
Photoreactive polymer
Phospholipid polymer
Photocleavable
Cell attachment
Cell detachment

ABSTRACT

Non-invasive and effective cell recovery from culture substrates is important for the passage and characterization of cells. In this study, a photoreactive polymer surface, which uses UV-irradiation to control substrate cell adhesion, was prepared. The photoreactive phospholipid polymer (PMB-PL) reported herein, was composed of a both 2-methacryloyloxyethyl phosphorylcholine (MPC) unit as a cytocompatible unit and methacrylate bearing a photolabile nitrobenzyl group. The PMB-PL polymer was used to coat a cell culture substrate thus affording a photoreactive surface. Surface analysis of the PMB-PL coating indicated a strong photoresponse owing to the sensitivity of the PL unit. Before light exposure, the PMB-PL surface provided cell adhesion. Following UV-irradiation, the PMB-PL coating was converted to a neutral ζ-potential and hydrophilic surface. The photoreactive surface conversion process allowed for the detachment of adhered cells from the PMB-PL surface while maintaining cell viability. This study demonstrates the promise and significance of the PMB-PL photoreactive surface as a method to control cell attachment and detachment for cell function investigation.

1. Introduction

Recently many researchers have shown interest in stimuli-responsive surfaces for cell engineering and other applications. The properties of such "smart surfaces" are effortlessly tuned using an external stimulus [1–5]. Control of cell attachment and detachment from a substrate with continued bioactivity is important for *in vitro* cell culture analysis. The stimuli-responsive surface properties that are of interest for cell engineering development include wettability, hydrophobicity, and hydrophilicity. Previously reported surfaces were responsive to electrical [6–9], temperature [10–12], pH [13–15], or light [16–18] external stimuli. Among the stimuli, light is regarded as ideal for increased spatial and temporal resolution control.

To achieve controlled cell attachment/detachment behavior under mild conditions, it is important to suppress non-specific biomolecule interactions. We have previously reported the 2-methacryloyloxyetyl phosphorylcholine (MPC) polymers that have excellent cytocompatibility due to the inhibition of non-specific biomolecule interactions [19]. These polymers have been widely applied in various fields within the life sciences, including the area of cell engineering materials [20–23]. The MPC polymers effectively suppress the typical inflammatory reaction of adhered cells [23]. Previously, a photo-functionalized MPC polymer bearing photoreactive moieties such as azidophenyl groups and photocleavable linkers were reported to prepare micropattern surfaces for cell adhesion control [24–27].

In this study, we prepared another photoreactive MPC polymer, which controls cell detachment using UV-irradiation. The 2-nitrobenzyl moiety is a typical photocleavable protective group for surface modification, which is cleaved by UV-irradiation ($\lambda = 365$ nm) using a mercury lamp [28]. Incorporating a photoreactive MPC polymer bearing a photocleavable (PL) monomer afforded the PMB-PL polymer. Upon UV-irradiation the cell adhesive molecules were converted at the PMB-PL surface and cell detachment was achieved. In this report, characterization of the PMB-PL polymer and cell attachment/detachment behavior at the surface were investigated.

2. Materials and methods

The MPC was purchased from NOF (Tokyo, Japan), which synthesized the product using the previously reported method [29]. Methacryloyl chloride was purchased from Wako Pure Chemical Industries, Ltd. (Osaka, Japan). The photolabile linker, 4-[4-(1-Hydroxyethyl)-2-methoxy-5-nitrophenoxy]butyric acid was purchased from Sigma–Aldrich Corp. (St. Louis, MO, USA). Other organic reagents were purchased with the highest available purity and were used without further purification.

* Corresponding author at: Department of Bioengineering, The University of Tokyo, 7-3-1, Hongo, Bunkyo-ku, Tokyo 113-8656, Japan.
E-mail address: konno@bioeng.t.u-tokyo.ac.jp (T. Konno).

0927-7765/$ – see front matter © 2011 Elsevier B.V. All rights reserved.
doi:10.1016/j.colsurfb.2011.08.029

HeLa (*Homo sapiens* epithelial cell line established from a uterine cervix carcinoma) and L929 cells (murine fibroblast cell line established from connective tissue) were purchased from Riken Cell Bank (Ibaraki, Japan). The cells were cultured in Dulbecco's Modified Eagle Medium, (DMEM Sigma, St. Louis, MO, USA) with 10% fetal bovine serum, (FBS, Invitrogen Life Technologies, Carlsbad, CA, USA).

2.1. Synthesis of the photocleavable monomer (PL)

The photocleavable monomer (PL) was synthesized under dark conditions using lightproof vials. The photolabile linker, 4-[4-(1-hydroxyethyl)-2-methoxy-5-nitrophenoxy]butyric acid (1.0 mmol) was dissolved in dry dichloromethane (DCM), which had been purged with Ar gas. Both triethylamine (TEA, 3.0 mmol) and methacryloyl chloride (MC, 2.5 mmol), were dissolved in dry DCM and added dropwise to the photolabile linker solution at 0 °C. The solution was stirred overnight at room temperature (RT). The stirred solution was washed with sodium bicarbonate (5%, w/v *aq*), dilute hydrochloric acid (1%, v/v *aq*), and water. The washed solution was evaporated and the remaining liquid product was dissolved in aqueous acetone (50%, v/v *aq*). The reaction mixture was stirred overnight at RT and the liquid monomer was extracted using DCM. The DCM layer was collected, washed with dilute hydrochloric acid (1% v/v, *aq*) and water, dried over magnesium sulfate, and evaporated to yield the photocleavable methacrylate monomer referred to as PL monomer. The structure of the PL monomer was confirmed using ^{1}H NMR (300 MHz, JEOL, Japan). The ^{1}H NMR chart and FT-IR spectrum of PL monomer was shown in Figs. S1 and S2, respectively.

^{1}H NMR (300 MHz, *DMSO-d6*): δ 12.3 (br, $CH_2COO\mathbf{H}$), 7.55 (s, Aromatic-**H**), 7.10 (s, Aromatic-**H**), 6.39, 6.05 (d, d, $OC(dO)CCH_3dC\mathbf{H_2}$), 5.3 (q, Aromatic-C**H**$(CH_3)OC(dO)CCH_3dCH_2$), 4.1 (t, Aromatic-O$\mathbf{CH_2}CH_2CH_2COOH$), 3.95 (s, Aromatic-O$\mathbf{CH_3}$), 2.5 (t, Aromatic-$OCH_2CH_2\mathbf{CH_2}COOH$), 2.1 (s, $OC(dO)CHdCH_2\mathbf{CH_3}$), 1.9 (m, Aromatic-$OCH_2\mathbf{CH_2}CH_2COOH$), 1.55 (d, Aromatic-$CHC\mathbf{H_3}$).

2.2. Synthesis of photocleavable phospholipid polymer (PMB-PL)

The photocleavable phospholipid polymer (PMB-PL) was synthesized via the conventional radical polymerization method using an α,α'-azobisisobutyronitrile (AIBN) initiator. The procedure was completed in a glass tube. The MPC (0.25 mol), BMA (0.50 mol), and photocleavable monomer (0.25 mol) were dissolved in a dioxane/ethanol mixture (1:1 by vol.) at a final concentration of 0.38 M. Thereafter, AIBN (0.38 mM) was added to the solution. The solution was purged with argon gas for 10 min and the glass tube was then sealed. The sealed tube was placed in an oil bath at 60 °C for 48 h. Following polymerization, the PMB-PL was precipitated from diethyl ether/chloroform (3:2 by vol.), and the solid product was collected. The PMB-PL solid was dried overnight, under reduced pressure.

The chemical structure of PMB-PL was confirmed using ^{1}H NMR (300 MHz, JEOL, Tokyo, Japan) and FT-IR (FT-IR 615, JASCO, Tokyo, Japan) spectroscopies. The molecular weight of PMB-PL was measured using a gel-permeation chromatography (GPC) system fitted with an OHpak SB-804HQ column (Shodex®, Showa Denko KK, Tokyo, Japan).

2.3. Surface characterization of PMB-PL

The glass cover slide (18 mm × 18 mm, thickness 0.12–0.17 mm, Matsunami, Tokyo, Japan) was cleaned using ultrasonication in hexane, ethanol, and chloroform solutions at RT for 20 min; then, the slide was treated with oxygen plasma. The glass slides were immersed in a 0.5% (w/v) PMB-PL ethanol solution, and were then dried under reduced pressure. To evaluate the photoreactive property of the PMB-PL surface, a UV-irradiation instrument (Spot-cure SP7, Ushio Inc., Tokyo, Japan) equipped with a 250-W UV lamp (UXM-Q256BY, Ushio Inc., Tokyo, Japan) was used. The power density of the UV source was 80 mW/cm^2.

Surface characterization of the PMB-PL coating was analyzed using Fourier transformed-infrared reflection adsorption spectroscopy (FT-IRRAS), X-ray photoelectron spectroscopy (XPS), static contact angle, ellipsometry, and surface ζ-potential measurement.

A FTIR-500 (JASCO, Tokyo, Japan) was used for the FT-IRRAS spectra measurement. The spectra were obtained under dry conditions at a resolution of 4 cm^{-1} and a scan number of 128.

The XPS spectra were measured using an AXIS-His instrument (Shimadzu/Kratos, Kyoto, Japan) equipped with a monochromatized, Mg-focused, X-ray source. High-resolution scans of C_{1s}, N_{1s}, O_{1s}, P_{2p}, and Si_{2p} were acquired at a photoelectron take-off angle of 90°. The energies in all spectra were corrected using the C_{1s} energy calibration peak at 285 eV.

Static water contact angle measurements were conducted at RT using a CA-W automatic contact-angle meter (Kyowa Interface Science, Tokyo, Japan). The water-in-air and air-in-water systems were applied in this study. In the water-in-air system, the typical protocol involved using a constant drop volume (200 μL) of ultra-pure water onto the surface. For the air-in-water system, the surfaces were horizontally submerged in ultra-pure water. Air bubbles were positioned on the undersides of the surfaces using a syringe equipped with a U-shaped needle. The water drops and air bubbles were monitored using a charge-coupled device (CCD) camera. The captured images were analyzed using FAMAS software (Kyowa Interface Science, Tokyo, Japan) to determine the static contact angle. The contact angle was calculated as the average of more than five values taken at different positions.

The thickness of the PMB-PL was measured under dry conditions using an ellipsometer (alpha-SE®, J.A. Woollam Co., Inc., Lincoln, NE, USA) with a He–Ne laser (632.8 nm) at a 70° incident angle. The refractive indices (n_r) of the Parylene C and poly(MPC) used in the measurement were 1.63 and 1.49, respectively, and both extinction coefficients (k_e) were 0.00. All measurements were conducted under RT air conditions. Data were collected at eight different locations from each sample.

The surface ζ-potential was measured in a 10 mM NaCl solution using a measurement unit (ELS-6000, Photal, Otsuka Electronics Co. Ltd., Osaka, Japan) with an ancillary flat plate cell (10 mm × 30 mm × 60 mm) coated with poly(acrylamide) at 25 °C. Polystyrene latex particles coated with hydroxypropyl cellulose were used as the mobility-monitoring particles.

2.4. Cell attachment/detachment at the PMB-PL surface

HeLa cells were cultured in a 100-mm cell culture dish at 37 °C in 5% CO_2 atmosphere using DMEM containing 10% FBS. After the cells reached sub-confluency, the old media was aspirated; the cells were rinsed with phosphate buffered saline (PBS) and then were exposed to trypsin (1 mL) for 2 min to detach the cells from the surface. The detached cells were added to fresh DMEM, and the cell suspension was centrifuged at 1000 rpm for 3 min. After centrifuging, the supernatant was aspirated and the HeLa cells were suspended in DMEM for the following experiments.

The PMB-PL coated cover-glass surfaces were placed into each well of a 24-well-plate cell-culture dish, sterilized with ethanol, and then washed with PBS. A cell suspension (2.0×10^4 cells/mL, 2 mL) was seeded on the PMB-PL surface and incubated under 5% CO_2 at 37 °C. After incubation for 4 h, unattached cells were washed off with warm fresh medium and the attached cells were observed